T07

hep-ex/0106100

Measurement of the Hadronic Cross Section at KLOE Using the Radiative Return

The KLOE collaboration
presented by Achim Denig
LNF - INFN, Frascati, Italy

We report on the measurement of the hadronic cross section below 1 GeV at the electron-positron-collider DAΦNE, using the multiple purpose detector KLOE. The radiative return, which is due to initial state radiation ($e^+e^- \to \gamma + hadrons$), allows us to obtain the cross section for *variable* center-of-mass-energies of the hadronic system from the $2m_\pi$ threshold up to 1.02 GeV. This measurement can be performed while DAΦNE is running with a *fixed* accelerator energy on the ϕ mass (1.02 GeV). For the exclusive process $e^+e^- \to \pi^+\pi^-\gamma$, the status of the analysis and first preliminary results of the invariant mass spectrum of the two-pion-state are presented.

1. HADRONIC CROSS SECTION AT DAΦNE

1.1. Motivation

The measurement of the hadronic cross section at low energies is of great importance for the improvement of the theoretical error of the anomalous magnetic moment of the muon, $a_\mu = (g_\mu - 2)/2$. The hadronic contribution $a_\mu^{\rm hadr}$ is given by the hadronic vacuum polarization and cannot be calculated at low energies in the framework of perturbative QCD. Following a phenomenological approach, the hadronic contribution can however be evaluated from the measurement of R through a dispersion relation.

$$a_\mu^{\rm hadr} = (\frac{\alpha m_\mu}{3\pi})^2 \int_{4m_\pi^2}^{\infty} ds \frac{R(s)\hat{K}(s)}{s^2}, \qquad (1)$$

where $R(s) = \frac{\sigma(e^+e^- \to \text{hadrons})}{\frac{4\pi\alpha^2(s)}{3s}}$ and the kernel $\hat{K}(s)$ is a smooth bounded function growing from 0.63 at threshold to 1 at ∞. Due to the $1/s^2$ dependence in the integral, hadronic data at low energies are strongly enhanced in the contribution to $a_\mu^{\rm hadr}$. The error of the hadronic contribution is therefore given by the limited knowledge of hadronic cross section data. This error is the dominating contribution to the total error of $a_\mu^{\rm theo}$ ($\delta a_\mu^{\rm theo} \approx \delta a_\mu^{\rm hadr}$).

We refer to [1], [2], [3] for a detailed discussion of the subject and the interpretation of the actual discrepancy between the theoretical and the experimental value for a_μ: $a_\mu^{\rm theo} = (11659159.7 \pm 6.7) \times 10^{-10}$ [2], $a_\mu^{\rm exp} = (11659202.0 \pm 15.0) \times 10^{-10}$ (world average including E821 measurement[1] [4]). In the value shown for $a_\mu^{\rm theo}$, τ decays have been included for the evaluation of the dispersion integral under the assumption of conserved vector current and isospin symmetry. The value for $a_\mu^{\rm hadr}$ under these assumptions is: $a_\mu^{\rm hadr} = (692.4 \pm 6.2) \times 10^{-10}$ [2]. An updated analysis [5], which includes e^+e^- *data only*, finds $a_\mu^{\rm hadr} = (697.4 \pm 10.5) \times 10^{-10}$, where the error can be reduced to $\approx 6 \times 10^{-10}$ if the hadronic cross section is measured with an accuracy of $\approx$ 1% in the energy range below 1 GeV.

*The KLOE collaboration: M. Adinolfi, A. Aloisio, F. Ambrosino, A. Andryakov, A. Antonelli, M. Antonelli, F. Anulli, C. Bacci, G. Barbiellini, F. Bellini, G. Bencivenni, S. Bertolucci, C. Bini, C. Bloise, V. Bocci, F. Bossi, P. Branchini, S. A. Bulychjov, G. Cabibbo, R. Caloi, A. Calcaterra, P. Campana, G. Capon, G. Carboni, A. Cardini, M. Casarsa, V. Casavola, G. Cataldi, F. Ceradini, F. Cervelli, F. Cevenini, G. Chiefari, P. Ciambrone, S. Conetti, E. De Lucia, G. De Robertis, R. De Sangro, P. De Simone, G. De Zorzi, S. Dell'Agnello, A. Denig, A. Di Domenico, C. Di Donato, S. Di Falco, A. Doria, E. Drago, O. Erriquez, A. Farilla, G. Felici, A. Ferrari, M. L. Ferrer, G. Finocchiaro, C. Forti, A. Franceschi, P. Franzini, M. L. Gao, C. Gatti, P. Gauzzi, A. Giannasi, S. Giovannella, V. Golovatyuk, E. Gorini, F. Grancagnolo, W. Grandegger, E. Graziani, P. Guarnaccia, H. G. Han, S. W. Han, X. Huang, M. Incagli, L. Ingrosso, Y. Y. Jiang, W. Kim, W. Kluge, C. Kuo, V. Kulikov, F. Lacava, G. Lanfranchi, J. Lee-Franzini, T. Lomtadze, C. Luisi, C. S. Mao, M. Martemianov, A. Martini, M. Matsyuk, A. Menicucci, W. Mei, L. Merola, R. Messi, S. Miscetti, A. Moalem, S. Moccia, M. Moulson, S. Müller, F. Murtas, M. Napolitano, A. Nedosekin, M. Panareo, L. Pacciani, P. Pagès, M. Palutan, L. Paoluzi, E. Pasqualucci, L. Passalacqua, M. Passaseo, A. Passeri, V. Patera, E. Petrolo, G. Petrucci, D. Picca, G. Pirozzi, M. Pollack, L. Pontecorvo, M. Primavera, F. Ruggieri, P. Santangelo, E. Santovetti, G. Saracino, R. D. Schamberger, C. Schwick, B. Sciascia, A. Sciubba, F. Scuri, I. Sfiligoi, J. Shan, P. Silano, T. Spadaro, S. Spagnolo, E. Spiriti, C. Stanescu, G. L. Tong, L. Tortora, E. Valente, P. Valente, B. Valeriani, G. Venanzoni, S. Veneziano, A. Ventura, Y. Wu, Y. G. Xie, P. F. Zema, P. P. Zhao, Y. Zhou

[1] The final goal of the E821 collaboration is a measurement of a_μ with a precision of ca. 4×10^{-10}

1.2. Radiative Return

We present in this paper a complementary approach for the measurement of the hadronic cross section, which uses the radiative process $e^+e^- \to hadrons + \gamma$, where the photon has been radiated by one of the initial electrons or positrons (Initial State Radiation, ISR) [6]. The DAΦNE collider is operating with a fixed center-of-mass-energy on the ϕ resonance[2]. Hence, the hadronic cross section in the energy range $(2m_\pi)^2 < Q^2 < (m_\phi)^2$ is accessible by *radiative return* (Q^2 is the invariant mass of the hadronic system). In order to deduce the differential cross section $d\sigma(e^+e^- \to \text{hadrons})/dQ^2$ from the measurement $d\sigma(e^+e^- \to \text{hadrons} + \gamma)/dQ^2$, a precise theoretical understanding of the initial state radiation process (radiation function H) is mandatory:

$$Q^2 \cdot \frac{d\sigma_{\text{hadrons}+\gamma}}{dQ^2} = \sigma_{\text{hadrons}} \cdot H(Q^2, \Theta_i). \qquad (2)$$

The knowledge of the function $H(Q^2, \Theta_i)$ (which depends on Q^2 and the experimental acceptance cuts Θ_i) at a precision better than 1% is a challenging task. However, radiative corrections were computed by different groups up to next-to-leading-order for the exclusive hadronic state $\pi^+\pi^-$ [7], [8], [9], [10]. We concentrated in our analysis on this important state ($e^+e^- \to \rho\gamma \to \pi^+\pi^-\gamma$) since it is the dominating hadronic reaction below the ϕ mass and the respective process $e^+e^- \to \rho \to \pi^+\pi^-$ accounts for 62% of the hadronic contribution to a_μ (see formula (1)).

We would like to stress that the radiative return method—as presented here—has the merit against the conventional energy scan, that the systematics of the measurement (for example, normalization, beam energy) have to be taken into account only *once* while for the energy scan they have to be known for *each* energy step.

1.3. Suppression of FSR

An important issue for the radiative return method is the suppression of events, where the photon has been emitted by one of the pions (Final State Radiation, FSR). The choice of a phase space region, where FSR is low, can reduce this kind of background to an acceptable limit. We found from Monte Carlo studies [11], that cutting on E_γ and Θ_γ (energy and polar angle of the photon) effectively suppresses FSR, while the ISR cross section remains high. ISR events are strongly peaked at small angles Θ_γ, while FSR events essentially follow the $\sin^2\Theta_\pi$ distribution of the pion tracks. It is therefore essential to measure $\pi^+\pi^-\gamma$ events with an upper acceptance cut for Θ_γ at small angles. A cut on E_γ additionally suppresses FSR due to the fact that the decay via the ρ resonance (that is, ISR) leads to an enhancement of the photon energy spectrum at $\approx 220MeV$ which is not visible in the case of FSR. For the following acceptance cuts—which are the ones used in our analysis—we find that FSR is suppressed below 1%:

$$5^o < \Theta_\gamma < 21^o, 159^o < \Theta_\gamma < 175^o \qquad (3)$$
$$E_\gamma > 10 \text{ MeV} \qquad (4)$$
$$55^o < \Theta_\pi < 125^o \qquad (5)$$
$$p_\pi^T > 200 \text{ MeV (transv. momentum)}. \qquad (6)$$

The effective cross section with these acceptance cuts is $4.2nb$. The description of FSR is model dependent and in the actual version of [8] a point like pion is assumed. The model dependence can be tested for $\pi^+\pi^-\gamma$ events by looking at the charge asymmetry of the produced pions:

$$A(\Theta_i) = \frac{N^{\pi^+}(\Theta_i) - N^{\pi^-}(\Theta_i)}{N^{\pi^+}(\Theta_i) + N^{\pi^-}(\Theta_i)}. \qquad (7)$$

This charge asymmetry arises from the interference between ISR and FSR and is therefore linear in the FSR amplitude. We

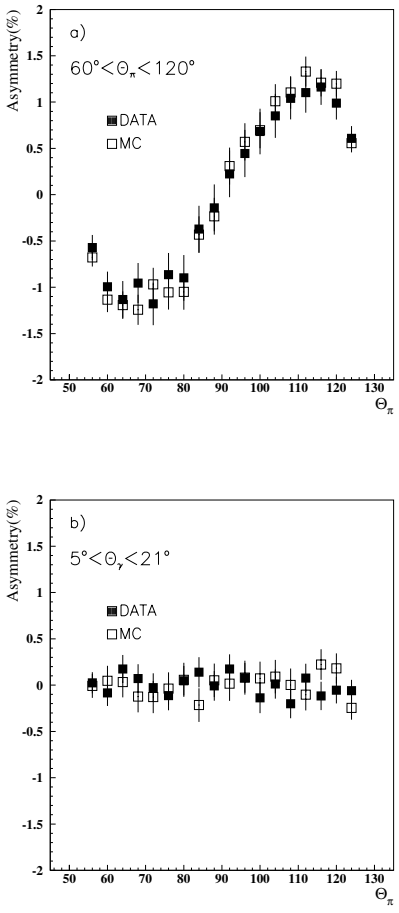

Figure 1: The charge asymmetry (formula (7)) is shown for 2 angular regions of the photon polar angle: (a) $60^o < \Theta_\gamma < 120^o$, where we see a sizable effect of the charge asymmetry due to larger FSR and (b) $5^o < \Theta_\gamma < 21^o$, where FSR and hence the charge asymmetry are small.

[2] An energy scan at DAΦNE requires a non trivial modification of the interaction region which has been designed especially for the ϕ mass region.

measured the charge asymmetry for (a) large photon angles ($60^o < \Theta_\gamma < 120^o$), where FSR is assumed to be large, and (b) for small photon angles ($5^o < \Theta_\gamma < 21^o$). The results are illustrated in Figure 1 and show a very good agreement between data and Monte Carlo, indicating that the point like model describes well the process of FSR within the error bars.

2. EVENT SELECTION

In this chapter we present the event selection for the measurement of the $\pi^+\pi^-\gamma$ final state. After a very brief description of the KLOE detector, the selection algorithm for this signal is presented.

2.1. The KLOE Detector

KLOE [12] is a typical e^+e^- multiple purpose detector with cylindrical geometry, consisting of a large helium based *drift chamber* (DC, [13]), surrounded by an *electromagnetic calorimeter* (EmC, [14]) and a superconducting magnet ($B = 0.6$ T). The detector has been designed for the measurement of CP violation in the neutral kaon system, that is, for a precise detection of the decay products of K_S and K_L. These are low momenta charged tracks ($\pi^\pm$, $\mu^\pm$, $e^\pm$ with a momentum range from 150 MeV/c to 270 MeV/c) and low energy photons (down to $20MeV$).

The DC dimensions (3.3 m length, 2 m radius), the drift cell shapes (2×2 cm^2 cells for the inner 12 layers, 3×3 cm^2 cells for the outer 46 layers) and the choice of the gas mixture (90% Helium, 10% Isobutane; $X_0 = 900$m) had to be optimized for the requirements prevailing at a ϕ factory. The KLOE design results in a very good momentum resolution: $\sigma_{p_\perp}/p_\perp \leq 0.3\%$ at high tracking efficiencies ($> 99\%$).

The EmC is made of a matrix of scintillating fibres embedded in lead, which guarantees a good energy resolution $\sigma_E/E = 5.7\%/\sqrt{E\,(\mathrm{GeV})}$ and excellent timing resolution $\sigma_t = 57ps/\sqrt{\mathrm{E(GeV)}} \oplus 50ps$. The EmC consists of a barrel and two endcaps which are surrounding the cylindrical DC; this gives a hermetic coverage of the solid angle (98%). However, the acceptance of the EmC below $\approx 20^o$ is reduced due to the presence of quadrupole magnets close to the interaction point and does not allow us to measure e.g. the photon of $\pi^+\pi^-\gamma$ events with low Θ_γ angles (as required for FSR suppression).

It will be shown in the following, that an efficient selection of the $\pi^+\pi^-\gamma$ signal is possible, without requiring an explicit photon detection. The relatively simple signature of the signal (2 high momentum tracks from the interaction point) and the good momentum resolution of the KLOE tracking detector allow us to perform such a selection.

2.2. Selection Algorithm

The $\pi^+\pi^-\gamma$ events are selected using the following 4 steps. The selection is based on the measurement of the charged pion tracks by the DC, while the photon is not required to be detected in the EmC. Calorimeter information is however used for the π/e-separation (likelihood method).

Charged vertex in DC

We require 1 vertex in the DC with 2 associated charged tracks close to the interaction point: $\sqrt{(x_V^2 + y_V^2)} \leq 8$ cm and $|z_V| \leq 15$ cm.

Likelihood Method for π/e-Separation

A fraction of radiative Bhabha events $e^+e^-\gamma$ enters the kinematical selection (see next selection cut), giving rise to a non negligible background. In order to reject those events, a likelihood method has been worked out for an effective π/e-separation. The method is based on the shape and energy deposition of the EmC clusters produced by the charged tracks and has been developed using independent control samples for the pion information ($\pi^+\pi^-\pi^0$ events) and for the electron information ($e^+e^-\gamma$ events). 98% of all $\pi^+\pi^-\gamma$ events are selected if at least one of the two tracks has been identified as a pion by the likelihood method. In Figure 2 the effect of the likelihood method is demonstrated in the track mass (M_{Track}) distribution[3]. $\pi^+\pi^-\gamma$ events are peaked at $M_{\mathrm{Track}} = m_\pi$, radiative Bhabha events at smaller values.

Kinematic Cut: 130.2 MeV < M_{Track} < 149.0 MeV

We perform a ± 9.6 MeV ($\pm 2\sigma$) cut on the kinematical variable M_{Track}, which is peaked at $M_{\mathrm{Track}} = m_\pi$ for $\pi^+\pi^-\gamma$ events (see again Figure 2). Background of $\pi^+\pi^-\pi^0$ events (with M_{Track} mostly > 150 MeV), $\mu^+\mu^-\gamma$ (with M_{Track} peaked at m_μ) and the bulk part of radiative Bhabha events $e^+e^-\gamma$ ($M_{\mathrm{Track}} < 100$ MeV) are mostly rejected (see subsection 3.1 on background).

Acceptance Cuts

The missing momentum of the 2 accepted charged tracks is calculated and associated with the photon under the assumption of a $\pi^+\pi^-\gamma$ event: $\vec{p}_\gamma^{\,DC} = \vec{p_\phi} - \vec{p_+} - \vec{p_-}$ [4]. The acceptance cuts of formulae (3)-(6) are then applied, where the photon related variables are taken from the DC missing momentum (photon is not explicitly measured).

---

[3] The M_{Track} variable is obtained solving the 4-momentum-conservation and resolving for the particle mass.

[4] $\vec{p_\phi}$ is the ϕ boost due to the beam crossing angle.

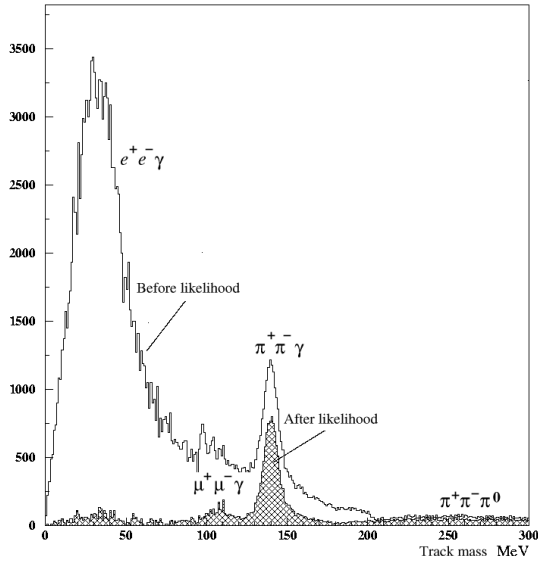

Figure 2: A likelihood method has been developed to separate electrons from pions. The kinematic variable track mass before and after the application of this method is shown. $\pi^+\pi^-\gamma$ events are peaked at $M_{Track} = m_\pi$, radiative Bhabha events at much smaller values. Other background channels are also visible ($\mu^+\mu^-\gamma$ and $\pi^+\pi^-\pi^0$).

3. EVENT ANALYSIS

The $\pi^+\pi^-\gamma$ cross section measurement contains the following terms:

$$\frac{d\sigma_{\text{hadrons}+\gamma}}{dQ^2} = \frac{dN_{\text{Obs}} - dN_{\text{Bkg}}}{dQ^2} \cdot \frac{1}{\varepsilon_{Sel}\varepsilon_{Acc}} \cdot \frac{1}{\int \mathcal{L}dt}. \quad (8)$$

It requires the study of the various background channels (N^{Bkg}, see following subsection), the selection efficiencies (ε_{Sel}) and the systematic effects due to the acceptance cuts applied (ε_{Acc}). Finally the counting rate measurement has to be normalized to the integrated luminosity $\int \mathcal{L}dt$ in order to achieve a cross section measurement. All these terms will be obtained from data.

Preliminary results concerning ε_{Sel} are presented in the following subsection. The detector smearing and the systematic effects, arising from there have been studied in detail from MC [11]. No limititations have been found for a high precision measurement on the percent level. However, more studies—including data—have to be done. We will also report on the KLOE luminosity measurement (Bhabha scattering at large angles).

3.1. Background

$e^+e^-\gamma, \mu^+\mu^-\gamma$

Radiative Bhabha events are mostly suppressed by the M_{Track} cut (chapter 2.2 (ii)). The remaining background due to events with a high value for M_{Track} and due to electrons, which had not been rejected by the likelihood method, is peaked at large Q^2 (above 0.7 GeV^2) and corresponds to a contamination below the percent level in this Q^2 region.

Events of the kind $\mu^+\mu^-\gamma$ are not efficiently rejected by the likelihood method, because they release energy in the EmC with a similar signature like pions. After the cuts of formulae (3)–(6) and after the M_{Track} cut, the remaining $\mu^+\mu^-$ cross section is low ($\approx 10^{-2} nb$), such that we expect only a small contamination ($< 1\%$ in the high Q^2 region > 0.7 GeV^2).

$\pi^+\pi^-\pi^0$

An important background for our signal is the decay $\phi \to \pi^+\pi^-\pi^0$ (B.R. 15.5%, $\sigma^{\text{tot}}_{\pi^+\pi^-\pi^0} \approx 500nb$). $\pi^+\pi^-\pi^0$ and $\pi^+\pi^-\gamma$ events are separated in the KLOE standard reconstruction scheme by a cut in the 2-dimensional plane $M_{\text{Track}} - Q^2$. At small Q^2, the M_{Track} values for the 2 channels are very similar and a part of the $\pi^+\pi^-\pi^0$ events appear as a background. The M_{Track} cut and the acceptance cut of formula (6) [5] reject a big part of these events.

In order to estimate from data the remaining contamination, we modified the standard cut in the $M_{\text{Track}} - Q^2$ plane by expanding the $\pi^+\pi^-\pi^0$ selection region. We see then the tail of $\pi^+\pi^-\pi^0$ events entering the M_{Track} selection interval. We perform this study in bins of Q^2. The $\pi^+\pi^-\pi^0$ background is negligible in most of the Q^2 region and gives only a contamination at the lower end of the spectrum between 0.3 GeV^2 and 0.4 GeV^2. The effective $\pi^+\pi^-\pi^0$ cross section after all the selection steps is $< 0.01nb$. It increases considerably if we select $\pi^+\pi^-\gamma$ events at larger polar angles of the photon.[6]

[5] The pion tracks have on the average a lower momentum as $\pi^+\pi^-\gamma$ events.

[6] This behaviour can be easily explained by the missing momentum of $\pi^+\pi^-\pi^0$ events (in this case the π^0), which is peaked at large angles.

3.2. Selection Efficiencies

We shortly summarize the various efficiencies which contribute to the total selection efficiency:

- Trigger: The trigger efficiency has 2 contributions: the probability of a $\pi^+\pi^-\gamma$ event to be recognized by the KLOE trigger (between 95% to 99% depending on Q^2) and the inefficiency which arises from a trigger hardware veto for the filtering of cosmic ray events. The second contribution causes an inefficiency for $\pi^+\pi^-\gamma$ events at large Q^2 (30% at 1 GeV^2) which decreases with lower Q^2 (fully efficient at ≈ 0.7 GeV^2). These values have been obtained from data by looking at the individual probabilities for π^+ and π^- to fire 1 trigger sector and 1 cosmic veto sector.
- Reconstruction Filter: A software filter is implemented in the KLOE reconstruction program for the filtering of non-collider physics events, like e.g. machine background and cosmic ray events. The inefficiency for $\pi^+\pi^-\gamma$ events caused by this filter is $\approx 2\%$ (taken from MC).
- Event Selection (see subsection 2.2): The DC vertex efficiency ($\approx 95\%$) is obtained from the Bhabha stream, which is selected without requiring DC information. The efficiency due to the likelihood selection is $\approx 98\%$ and is evaluated from data during the construction of the likelihood method. The efficiency due to the $M_{\rm Track}$ cut ($\approx 90\%$) is evaluated from Monte Carlo at present.

3.3. Luminosity Measurement

The DAΦNE accelerator does not have luminosity monitors at small angles (like, for example, LEP) due to the existence of focusing quadrupole magnets very close to the interaction point. The luminosity is therefore measured using large angle Bhabha (LAB) events, for which the KLOE detector itself can be used. The effective Bhabha cross section at large angles ($55^o < \Theta_{+,-} < 125^o$) is still as high as $425nb$. The number of LAB candidates N_{LAB} are counted and normalized to the effective Bhabha cross section, obtained from Monte Carlo:

$$\int \mathcal{L}dt = \frac{N_{\rm LAB}(\Theta_i)}{\sigma^{MC}_{\rm LAB}(\Theta_i)} \cdot (1 - \delta_{\rm Bkg}). \qquad (9)$$

Hence, the precision of this measurement depends on:

- the theoretical knowledge of the Bhabha scattering process including radiative corrections;
- the simulation of the process by the detector simulation program.

For the theory part we are using 2 independent Bhabha event generators (the Berends/Kleiss [15] generator, modified for DAΦNE in [16] and BABAYAGA [17]).

We use a selection algorithm for LAB events with a reduced number of cuts, for which we expect a very good description by the KLOE detector simulation program. The acceptance region for the electron and positron polar angle ($55^o < \Theta_{+,-} < 125^o$) is measured by the EmC clusters produced by these tracks, while the energy measurement ($E_{+,-} > 400$ MeV) is performed by the high resolution drift chamber. Taking the actual detector resolutions, we expect the systematic errors arising from these cuts to be well below 1%. Moreover, the background from $\mu^+\mu^-(\gamma)$, $\pi^+\pi^-(\gamma)$ and $\pi^+\pi^-\pi^0$ is cut to a level below 1% and can be easily subtracted. All the selection efficiencies concerning the LAB measurement (Trigger, EmC cluster, DC tracking) are above 98% and are well reproduced by the detector simulation.

As a goal we expect to measure the DAΦNE luminosity at the level of 1%. The very good agreement of the experimental distributions ($\Theta_{+,-}$, $E_{+,-}$) with the existing event generators and a cross check with an independent luminosity counter based on $e^+e^- \to \gamma\gamma(\gamma)$, indicate a good precision. However, more systematic checks (e.g. the effect of a varying beam energy and of a non centered beam interaction point) are still to be done.

3.4. Comparison with Monte Carlo

We analyzed a data sample of $16.4\,pb^{-1}$ and present in Figure 3 the preliminary result for the differential cross section $d\sigma(e^+e^- \to \pi^+\pi^-\gamma)/dQ^2$. The plot shows the *effective* cross section after all acceptance cuts (formulae (3) to (6)). The solid line is the prediction of our $\pi^+\pi^-\gamma$ event generator ([8], called EVA) after the detector simulation and after the correction for the various selection efficiencies (see subsection 2.2). Up to $Q^2 \approx 0.9$ GeV^2 we obtain an overall good agreement between data and MC. The deviation for $Q^2 > 0.9$ GeV^2 is due to a systematic effect connected with the definition of the fiducial volume for Θ_γ. This deviation will disappear by moving the lower border of the fiducial volume from 5^o to 0^o (not possible with the actual version of the event generator; see summary chapter).

The statistical error of the data points in the ρ peak region is $\approx 2\%$. The actual version of the event generator has a systematic uncertainty of the same size. By comparing the data and MC distributions we conclude that the accuracy of our cross section measurement is on the level of a few percent, which will be considerably improved with the ongoing analysis.

4. SUMMARY AND OUTLOOK

We presented in this paper the measurement $d\sigma(e^+e^- \to \pi^+\pi^-\gamma)/dQ^2$ for $Q^2 < 1$ GeV^2 using the radiative return method. The data sample[7] ($16.4\,pb^{-1}$) shows a good agreement with the existing event generator. We conclude that the experimental understanding of efficiencies, background and

[7] This corresponds to about one half of the full data set which KLOE has taken in 2000.

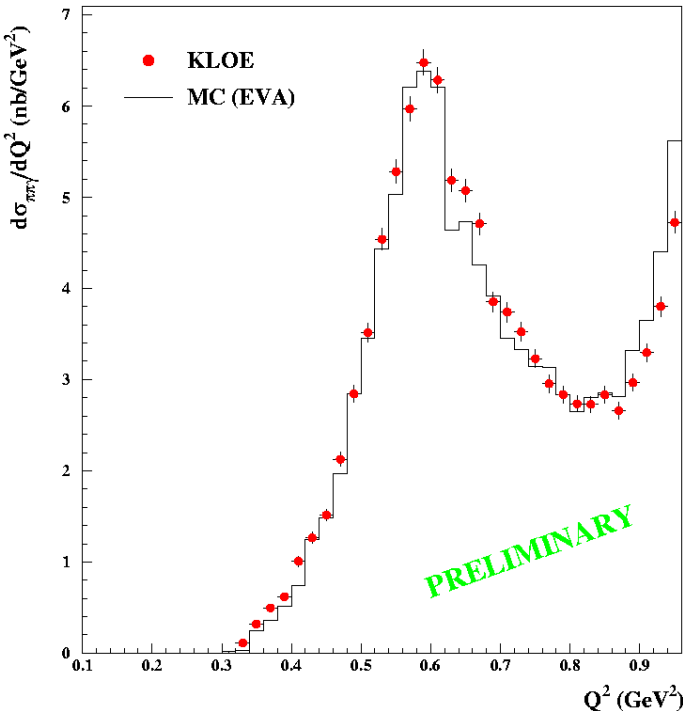

Figure 3: The differential $\pi^+\pi^-\gamma$ cross section as a function of the pion invariant mass. The solid line is the prediction of the theoretical event generator EVA of [8].

luminosity are well under control. We further conclude that the radiative return is a competitive method to measure hadronic cross sections, while the center-of-mass-energy of the accelerator is fixed. This could be proved for the first time in a systematic way with the results presented in this paper.

Data has been taken as a by-product of the KLOE ϕ physics program and no specific runs were necessary to perform this measurement. We stress the advantage of the radiative return, that systematic errors, like luminosity and beam energy, enter only once in this case and do not have to be known for individual energy points.

For the future we plan to refine the actual analysis and to change the acceptance cut for the photon polar angle from 5^o to 0^o. A comparison with MC will be possible in this case with the new next-to-leading-order event generator [9] and will improve the precision of the measurement due to a better systematic control of the fiducial volume. Also from the statistical point of view this modification will be helpful, since it corresponds to an increase of the effective $\pi^+\pi^-\gamma$ cross section of almost a factor 4.

Moreover we are studying the possibility to enlarge the acceptance region for $\Theta_{+,-}$, which increases the kinematical acceptance of events at low Q^2 (< 0.3 GeV^2).

In order to improve on a_μ^{hadr} and to be competitive with results coming from the CMD-2 experiment in Novosibirsk [18], a final precision for this measurement on the percent level is needed. A statistical error on this level is achieved with a total data sample of $\approx 200 pb^{-1}$ which is in reach for the months to come[8].

We are also investigating the possibility to perform an *inclusive measurement* $d\sigma(e^+e^- \to \pi^+\pi^-(n\gamma))/dQ^2$ without any cut on the number nor on the kinematics of photon(s). The radiative corrections for such a measurement are calculated with high precision ($< 1\%$) and will allow to extract the pion form factor more precisely. The background suppression ($\pi^+\pi^-\pi^0$) and the understanding of FSR need further experimental and theoretical investigations.

REFERENCES

[1] S. Eidelman and F. Jegerlehner, Z.Phys. C **67** (1995) 585
[2] M. Davier and A. Höcker, Phys.Lett. B **435** (1998) 427
[3] W.J. Marciano and B.L. Brown, [hep-ph/0105056]
[4] H.N. Brown *et al.* [E821 collaboration], Phys.Rev.Lett. **86** (2001) 2227
[5] F. Jegerlehner, [hep-ph/0104304]
[6] S. Spagnolo, Eur. Phys. J. C **6** (1999) 637
[7] V.A. Khoze, M.I. Konchatnij, N.P. Merenkov, G. Pancheri, L. Trentadue, O.N. Shekhovyova, Eur. Phys. J. C **18** (2001) 481
[8] S. Binner, J.H. Kühn, K. Melnikov, Phys.Lett. B **459** (1999) 279

[8]The DAΦNE performance at the moment (June 2001) is $> 1 pb^{-1}$ per day.

[9] G. Rodrigo, A. Gehrmann-De Ridder, M. Guilleaume, J.H. Kühn, [hep-ph/0106132]
[10] K. Melnikov, F. Nguyen, B. Valeriani, G. Venanzoni, Phys.Lett. B **477** (2000) 114
[11] A.Denig, Proceedings to *DAΦNE'99*, **Frascati Physics Series XVI** (2000) 569
[12] A. Aloisio *et al.* [KLOE collaboration], *The KLOE Detetor, Technical Proposal*, **LNF-93/002** (1993)
[13] M. Adinolfi *et al.* [KLOE collaboration], *The Tracking Detector of the KLOE Experiment*, **LNF-01/016** (2001); to be published in Nuclear Instruments and Methods
[14] M. Adinolfi *et al.* [KLOE collaboration], *The KLOE electromagnetic calorimeter*, **LNF-01/017** (2001); to be published in Nuclear Instruments and Methods
[15] F.A. Berends, R. Kleiss, Nucl.Phys. B **228** (1988) 537
[16] E. Drago, G. Venanzoni, *A Bhabha Generator for DAΦNE including radiative corrections and ϕ resonance*, **INFN/AE-97/48** (1997)
[17] C.M.C. Calame, C. Lunardini, G. Montagna, O. Nicrosini, F. Piccinini, Nucl. Phys. B **584** (2000) 459
[18] R.R. Akhmetshin *et al.* [CMD-2 collaboration], [hep-ex/9904027]